

Original Article

Finite Element Investigation of Reinforced Concrete Flat Slab-Column Connections under Static and Seismic Loading

Vinodkrishna M Savadi^{1,3,4*}, Santosh M Muranal², Sreeshail Heggond³

¹Department of Civil Engineering Acharya Institute of Technology, Bangalore, Karnataka, India.

²Department of Civil Engineering, Amrutha Institute of Engineering and Management Science, Bidadi, Karnataka, India.

³Department of Civil Engineering, Basaveshwar Engineering College, Bagalkot, Karnataka, India.

⁴Visvesvaraya Technological University, Belagavi, Karnataka, India.

*Corresponding Author : Vinodkrishnams@gmail.com

Received: 11 November 2025

Revised: 15 December 2025

Accepted: 12 January 2026

Published: 14 January 2026

Abstract - Punching Shear failure is a severe Limit condition that controls the seismic behavior of Reinforced Concrete (RC) flat slab-column connections. Such critical structural connections are widely used in modern construction due to economic design benefits and aesthetic appearances, which reduce the floor height in the absence of beams. The study identifies the key parameters that influence flat slab column connection failures, including punching shear, inadequate reinforcement, and poor detailing. Previous studies have revealed that the punching shear failure is the primary cause of Flat slab column connection failures, strongly influenced by concrete grade and reinforcement detailing. This work is a Finite Element Analysis (FEA) exploration of twelve flat slab-column connection models in FEA software to assess the effect of concrete grades M25 and M30, utilizing different types of reinforcement, including stirrups and stud rails, and loading for both static and seismic conditions. Concrete Damaged Plasticity (CDP) was used to model the nonlinear material behaviour of concrete, and the seismic shear demand was applied as required by the IS 1893. Unstiffened flat slabs in the shear region were brittle and exhibited rapid post-peak strength that declined, resulting in low residual capacity. Conversely, a stiffened flat slab in the shear region has demonstrated significant improvements in mass-carrying capacity, ductility, and energy-dispersing capabilities. Stirrups increased confinement, and stud rails offered better stability at the post-peak by maintaining residual strength and increasing the time to evolve damage. A higher concrete grade increased stiffness and maximum resistance, whereas the type of reinforcement was a key factor in determining ductility. A relative comparison with IS 456, ACI 318, and Eurocode 2 design provisions revealed that the predictions of punching shear using these codes are always conservative compared to those obtained through numerical methods. In general, the results emphasize the significance of reinforcement detailing in increasing the seismic resilience of flat slab systems, with stud rails proving to be the most promising form of reinforcement.

Keywords - Reinforced Concrete (RC) slab-column connections, Punching shear, Finite Element Analysis (FEA), Concrete Damaged Plasticity (CDP), Seismic performance, Shear reinforcement, Stirrups, Stud rails, Ductility, Residual strength, Flat slab systems.

1. Introduction

Modern reinforced concrete structures frequently use flat slab systems because of their effective usage of space, minimal formwork, architectural flexibility, and ease with which they can be routed with utilities. However, the flat slab column connections are likely to collapse in brittle punching failure, particularly in combined gravity and seismic loading. The absence of beams and insufficient shear reinforcement in flat slab column connections results in excessive serviceable residual deformation, which is a severe safety and serviceability problem in the event of lateral drifts. The study focuses on the resilient design of improving the knowledge of

the effect of concrete grades, reinforcement detailing, and loading protocols (Static vs seismic) in the load deformation behaviour, damage development, and ultimate strength.

1.1. Significance of Flat Slab-Column Connections: Historical Context and Seismic Challenges

Flat slab construction can be traced to the first half of the twentieth century, when C. A. P. Turner (1905-1909) developed the so-called muscle of construction known as the mushroom flat slab system, allowing direct transmission of the slab's load to beamless, column-supporting structures. The innovation was a major breakthrough in the design of



reinforced concrete and resulted in the popularization of flat slabs in structures that needed large open areas. The Marshall Building (1906) is frequently mentioned as one of the first extant examples of such a system, which proves its structural relevance over a long period of time [1]. Although the slab-column connection is more than 100 years old, it has been a significant vulnerability of the flat slab systems. Slab-column connections, as opposed to beam-column joints, are required to resist vertical shear, unbalanced bending, and torsional forces in a small area. Given the lateral drift during the seismic, the connection experiences unbalanced moments that are cyclic, which augments the demand on the punching shear, accelerating crack propagation. According to the reports on historical destruction of earthquakes, such as the destruction of Mexico City (1985) and other seismic events, flat slabs were severely damaged or collapsed due to punching failures at the slab-column joints [2].

Current seismic design codes are aware of this weakness and still employ simplified empirical formulations that fail to include the full three-dimensional stress transfer, post-cracking behavior, and confinement effects. This has made the seismic behavior of the flat slab-column connections challenging to predict precisely, which requires sophisticated analytical and numerical studies to assist in the implementation of safer design engineering.

1.2. Punching Shear Failures and Comparison with Other Connection Types

The nature of punching shear failure in flat slab-column connections is quite different from other failure modes in the beam-supported slab system or beam-column joints. Beams in framed systems spread the weight of gravity and lateral forces, permitting flexural yielding and ductile energy loss to take place at non-critical joints. By comparison, flat slab systems pass the forces through slab-column assemblages, leading to very localized shear forces and a tendency towards brittle punching failure unless sufficient reinforcement is included. Recent research has pointed out that slab-column associations without shear reinforcement have only a small rotative ability and a sharp reduction in post-peak strength under seismic effects.

Relative to beam-slab systems, the ductility of beam-slab has been shown to be better, where plastic hinges develop in the beam instead of brittle shear at the joints. This natural variation renders flat slab systems more sensitive to seismic requirements and places more emphasis on connection detailing. The modern studies of the punching shear failures have widened over the past years. A study by Utkarsh et al. (2025) points to a swift increase in publications on the topic of the punching shear mechanisms, reinforcement strategies, and numerical modelling techniques [3]. Classen (2023) suggested a framework based on response theory to enhance the mechanistic insights of the punching shear behaviour as opposed to the empirical code equations. Both experimental

and numerical studies have also shown that vertical shear reinforcement, including closed stirrups or headed stud rails, can cause a substantial change in crack paths, slow the onset of punching cones, and increase the residual strength [4].

Flat slab-column connections require special reinforcement techniques in comparison to other types of connections to obtain similar seismic integrity. Thus, the knowledge of punching shear behavior and reinforcement efficiency in flat slab systems is still paramount in the assurance of structural safety during seismic activities.

1.3. Influence of Concrete Grade

Experiments on the high-strength or ultra-high-performance concretes indicate that concrete grade was a significant factor affecting stiffness, cracking, and final shear load. To illustrate, the UHPC studies (Liu et al., 2025) recommend that augmenting the concrete strength elevates the initial stiffness and the cracking load, the ultimate load, and better flexural strength in most instances [5]. Also, by studies of High-Strength Concrete (HSC) slab-column connection under cyclic or monotonic load, e.g., in Punching Shear behavior of HSC Slab-Column Connection Under Cyclic loading, it is confirmed that HSC increases capacity and stiffness but can decrease drift capacity under lateral loading when not reinforced appropriately [6].

1.4. Effect of Reinforcement Type (Stirrups and Studs)

Modern construction greatly benefited from reinforced concrete flat slab systems due to their architectural flexibility, reduced cost of formwork, and the ease with which they can be routed with utilities. Nevertheless, the connections of slab-column in such systems are likely to collapse in brittle punching shear failure, particularly in combined gravity and seismic loading. Absence of beam support and insufficient shear reinforcement can consequently result in spontaneous collapse or excessive serviceable residual deformation, which is a severe safety and serviceability problem in the event of lateral drifts. Therefore, the resilient design should focus on improving the knowledge of the effect of the concrete grade, reinforcement detailing, and loading protocol (static vs seismic) in the load deformation behaviour, damage development, and ultimate strength.

Comparison of various shear reinforcement systems has been carried out in terms of the performance of traditional stirrups, stud rails (headed studs), and other sophisticated designs. Maues et al. (2025) compared headed studs with traditional stirrups and found that headed studs had better strength and ductility with the same amount of shear reinforcement [7]. Likewise, in the experimental study on punching shear strength of slab column connections in RC flat plate by Lim (2025), it was established that slabs reinforced by shear studs or shear stud rail had much higher punching shear resistance than slabs reinforced by stirrup, despite their being reinforced by the same geometrical conditions [8].

Experimental and numerical studies have recently achieved a lot in this field. Maués et al. (2025) numerically simulated flat slabs with different numbers of double-headed studs and closed stirrups and concluded that headed studs are superior to conventional shear links in terms of post-peak ductility and crack behaviour [7].

Liu et al. (2025) focused on the experimental study of Ultra-High-Performance Concrete (UHPC) slabs, revealing a certain slab thickness (around 100 mm) beyond which the behaviour of punching shear changes considerably, and steel fibres improve the behaviour of cracking and ultimate loads [9]. The comparison of strengthening methods of flat slabs with shear reinforcement, flexural reinforcement, and external strengthening (FRP, bolts) confirmed that well-anchored shear reinforcement offers enormous benefits in terms of strengthening and deformation capacity [10].

The ML models used by Zheng et al. (2024) showed that effective depth and reinforcement layout are influential factors that determine the punching shear strength of FRP-RC slabs, and the current design codes cannot explain these interactions with enough precision [11]. Ors et al. (2024) created correction factors of ACI-318 and EC2 to post-tensioned UHPC slabs based on ML techniques, which further confirms that the current code estimates are usually conservative [12].

Evolution of damage, residual strength, and ductility has also been addressed in numerous works. Yan and Xie (2024) came up with ML-driven predictions that indicate that the residual capacity and the progression of damages are very sensitive to the parameters such as the ratio of reinforcement, the quality of concrete, and the loading protocol [13]. The post-cracking behaviour and damage mitigation of slabs reinforced with fibre-reinforced concrete or fibre-reinforced polypropylene reinforcements are improved studies [3, 10].

Although there have been notable gains in the study of slab-column connections, there is limited literature that directly compares stirrups and stud rails under the same geometrical and loading conditions. Residual strength, ductility, and the progression of damage under seismic loading have had limited focus, and the effects of increased concrete grade and type of reinforcement are not yet fully investigated. In addition, the comparison with major design standards, including IS 456, ACI 318, and Eurocode 2, is frequently absent, making such standards less practical.

In order to fill these gaps, the current paper constructs a set of finite element models in FEA software through the Concrete Damaged Plasticity (CDP) framework to assess the impact of concrete grade (M25, M30), reinforcement type (none, stirrups, stud rails), and loading regime (static, seismic). These include the nonlinear load-deformation response assessment, the strength and ductility nature, redistribution of stress and damage processes, and

benchmarking the results to the predicted code-based punching shear results in an effort to suggest design-oriented developments to the resilient flat slab structures.

1.6. Research Gaps and Rationale for the Present Study

Despite the previous extensive experimental and numerical studies on the Reinforced Concrete (RC) flat slab-column connections, there are still a number of gaps of critical nature in the analytical understanding of the behaviour of these connections when subjected to gravity and seismic loads together.

First, the majority of the literature examines either gravity-dominated punching shear behaviour or isolated cyclic loading conditions, but the interaction between sustained gravity loads and subsequent seismic actions in the lateral direction is seldom studied within a single framework. This restricts the capability to clearly determine the stiffness degradation, residual strength, and the post-peak stability of slab-column connections subjected to earthquake demands.

Second, the proposals of available designs, such as IS 456:2000, ACI 318-19, and Eurocode 2, mainly rely on empirical formulations that have been formulated using simplified assumptions based on experimental databases. Not explicitly modelled in these code expressions are three-dimensional stress transfer, confinement effects, and the redistribution of stresses in the aftermath of cracking, as well as the effects of reinforcement detailing during seismic actions. As a result, large deviations between codal predictions and experimental structural behaviour have been noted, mainly in reinforced slab–column connections.

Third, although nonlinear finite element analysis has been used in a number of numerical studies to investigate punching shear, there are no validated and systematically calibrated models that can reproduce the evolution of damage, cyclic degradation, and failure mechanisms under seismic loading. Specifically, the synergistic effect of the reinforcement configuration, concrete grade, and loading protocol on ductility and residual capacity remained unquantified in an exhaustive manner.

Fourth, the literature data on closed stirrups and the headed stud rails are predominantly tested as separate shear reinforcement systems or in varying geometry and material settings. There are limited direct comparative studies of stirrups and stud rails at the same slab geometry, concrete grade, ratio of reinforcement, and seismic loading conditions, particularly in numerical studies of post-peak behaviour and damage progression.

Lastly, nonlinear finite element outcomes are often not systematically benchmarked against a variety of international design codes. The majority of the works compare findings with one code, or discuss only strength prediction, and little is

said about codal conservatism, implications of ductility, or seismic design adequacy.

2. Differentiation and Contributions of the Present Study

- In order to fill the above gaps, the current study clearly separates itself from the previous research in the following ways:
- A nonlinear finite element model, called Concrete Damaged Plasticity (CDP), is established to simulate the behaviour of flat slab-column connections due to combined gravity and seismic loading, and capture the behaviour of the connections, including cracking, crushing, degradation of stiffness, and post-peak behaviour.
- Unstiffened, stirrup-reinforced, and stud-rail-reinforced slab-column connections under the same geometry, reinforcement layout, concrete grade (M25 and M30), and loading protocols are systematically and directly

compared, and this allows an unbiased evaluation of the reinforcement efficiency.

- The work clearly analyses residual strength, ductility, and progression of damage, transcending peak-load comparisons and giving us an idea of seismic resilience and post-peak stability.
- Numerical predictions are performed and benchmarked against IS 456, ACI 318, and Eurocode 2, indicating codal conservatism, limitations, and implications of seismic design.
- Interaction of concrete grade with reinforcement detailing is measured, thus explaining the argument whether material strength can alone increase seismic performance or whether it should be supplemented with efficient confinement systems.

For clarity and systematic evaluation, twelve numerical models (C1–C12) are classified into three groups, with each group examined under both static and seismic loading for two concrete grades (M25 and M30), as summarized in Table 1.

Table 1. Classification of flat slab–column connection specimens

Group	Specimens	Reinforcement Type	Concrete Grade	Loading
C1–C4	Conventional (Unstiffened)	—	M25, M30	Static & Seismic
C5–C8	Stiffened with Stirrups	Stirrups	M25, M30	Static & Seismic
C9–C12	Stiffened with Stud Rails	Stud Rails	M25, M30	Static & Seismic

The given classification system in Table 1 helps to evaluate the non-linear behaviour of flat slab-column connections in different concrete grades, reinforcement, and loading factors in a systematic way. The conventional unstiffened flat slab column models (C1–C4) are used to come up with the baseline strength, stiffness, and failure mechanisms. This is for the purpose that the contribution of shear reinforcement to confinement and energy dissipation is measured by the stiffened flat slab column with stirrup-reinforced group (C5–8), and the effectiveness of the advanced reinforcement systems in controlling the crack propagation and post-peak load resistance is measured by the stiffened flat slab column with stud-rail-reinforced group (C9–12). This classification enables the in-depth assessment of the integrated effect of material strength, reinforcement detailing, and loading conditions on ductility, residual capacity, and code compliance, considering two grades of concrete (M25 and M30) under static and seismic loading.

2.2. Problem Definition and Unique Insights of the Present Study

2.2.1. Research Problem Definition

Although reinforced concrete flat slab systems are fully employed, the seismic characteristics of slab-column connections are poorly known, especially regarding the punching shear strength at combined gravity and lateral loads. Available studies and design codes are mostly concerned with punching shear using strength-based empirical equations,

which fail to capture the three-dimensional stress field, cyclic degradation, confinement effects, and redistribution of margin loads after reaching the peak that dominate failure in seismic events.

Moreover, in existing studies, it is not made clear:

- How various shear reinforcement systems (stirrups and stud rails) behave at the same geometry, material characteristics, and seismic loading regimes, and
- Whether or not a concrete grade increase can effectively enhance seismic performance without corresponding reinforcement details.

Consequently, designers are provided with no quantitative information regarding the relative effectiveness of reinforcement strategies in increasing ductility, residual strength, and damage control in flat slab-column connections subjected to seismic demand. The result of this gap is either excessively safe designs or, on the other hand, excessively unsafe over-reliance on concrete strength, which is especially common in areas of moderate-to-high seismicity.

As such, the research problem specific to the current study is: What is the interaction between concrete grade and shear reinforcement detailing and its effect on punching shear behaviour, ductility, damage growth, and residual capacity of flat slab-column connections under combined gravity and seismic loading, and how well current design codes reflect this behaviour?

2.2.2. Unique Insights and Contributions of the Study

The current research offers clear and new knowledge over the literature in the following ways:

Comparisons of reinforcement systems are direct and in control

Compared to the previous research, which evaluated stirrups or stud rails separately, this study will compare unstiffened, stirrup-reinforced, and stud-rail-reinforced slab-column connections under the same geometry, concrete grade, reinforcement pattern, and loading, and isolate the actual role of the reinforcement type.

Beyond peak strength seismic performance

The work evaluates not only ultimate punching capacity but also ductility, residual strength, post-peak stability, and damage evolution, which are important to seismic resilience yet seldom measured in numerical studies.

Connection of concrete grade and reinforcement detailing

Through testing of two concrete grades (M25 and M30), the investigation shows that increased concrete strength enhances stiffness and peak capacity, but does not replace a good shear reinforcement, giving an insight into a design assumption that is misunderstood.

Damage Modelling is Theoretically Realistic and Nonlinear

A calibrated CDP framework is used to model cracking, crushing, stiffness degradation, and cyclic damage development, which provides a more realistic model of slab-column behaviour under seismic loading.

Holistic Codal Benchmarking

The numerical findings are compared systematically with the IS 456, ACI 318, and Eurocode 2, showing the degree of conservatism, weaknesses of the existing provisions, and failure of codes to completely reflect the improved performance of stud-rail systems.

Seismic Flat Slab Design-Relevant Conclusions

The results present a well-defined, mechanism-based recommendation of reinforcement strategies to be applied to seismic flat slab structures, outlining stud rails as the most effective solution to accomplish increased ductility, damage control, and residual capacity.

3. Methodology

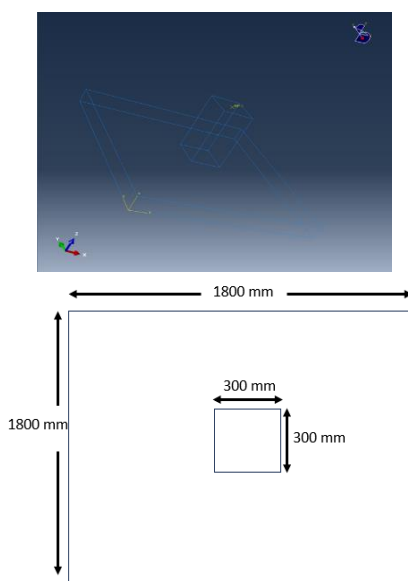
The methodology involves analytical investigations using FEA Software to evaluate the behaviour of flat slab column connections. Specimens with varying concretes and reinforcement types were tested under static and seismic loads to assess the punching shear resistance and structural performance.

The commercial finite element software Abaqus/CAE with the Abaqus/Standard implicit solver was used to perform

all the numerical simulations. The modelling framework was created to represent the nonlinear punching shear behaviour of flat slab column connections based on material nonlinearity and the development of damage. The Concrete Damaged Plasticity (CDP) model was used to describe tensile cracking, compressive crushing, stiffness degradation, and post-peak behaviour, and to represent reinforcing steel as an elastic-plastic material with isotropic hardening. Embedded region constraints were assumed to establish a perfect bond between concrete and reinforcement; the method is widely applied to comparative studies of slabs and columns when bond-slip data are not available. The choice of concrete grades M25 and M30 indicates the popular grades in Indian building practice and allows determining whether the moderate increase of strength is sufficient to improve seismic performance or should be accompanied by shear reinforcement. To describe baseline behaviour, conventional strengthening, and advanced punching shear reinforcement, three reinforcement configurations, namely, unstiffened, closed stirrups, and stud rail, were employed. The parameter matrix was determined by changing the concrete grade and type of reinforcement, loading protocol (static or seismic), and keeping geometry, boundary conditions, and modelling assumptions fixed, thus isolating the contribution of each parameter to punching shear resistance, ductility, evolution of damage, and residual strength.

3.1. Geometry and Discretisation

All models were composed of a flat slab with dimensions of $1800 \times 1800 \times 150$ mm with a centrally located square column stub that measures $300 \times 300 \times 500$ mm in size. Deeply discretised reduced-integration C3D8R hexahedral elements were used to discretise the connection region, with mesh refinement of about 25 mm in the proximity of the slab-column interface and fewer elements in the further areas (Figure 1).



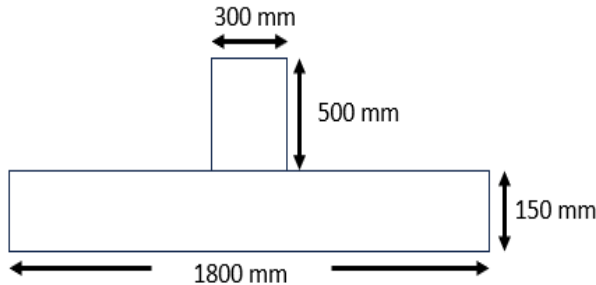


Fig. 1 Geometry of slab–column connection model
(slab: $1800 \times 1800 \times 150$ mm; column: $300 \times 300 \times 500$ mm)

3.2. Material and Reinforcement Modelling

Concrete was modelled based on grade-dependent elastic behaviour: M25 and C35 as tabulated in Table 2. The CDP compression hardening, tension stiffening, and damage evolution parameters of the literature were used to incorporate nonlinearity. The modelling of reinforcing steel was elastic-plastic. The embedded truss elements of T3D2 type were used as shear reinforcement with two layouts: closed stirrups that were concentrically built around the column and parallel stud rails (Figure 2(a) and (b)) spaced at 150 mm.

Table 2. Material reinforcement properties

Material	Elastic Modulus (E, GPa)	Poisson's Ratio (v)	Density (ρ , kg/m ³)
Concrete(M25)	30	0.2	2400
Concrete (C30)	34	0.2	2400
Reinforcing Steel (Fe-415)	200	0.3	7850

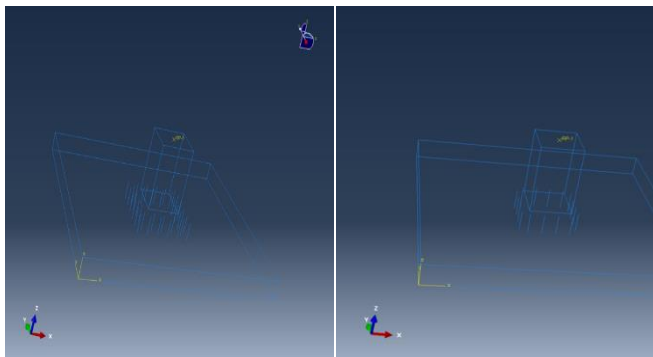


Fig. 2 Reinforcement layouts, (a) Closed stirrups, and (b) Stud rails at 150 mm spacing.

3.3. Boundary Conditions and Coupling

The edges of slabs were clamped to prevent translation but allowed rotations, which allows model continuity with the adjacent panels as shown in Figure 3.

The column bottom was attached to provide a simulation of lower-story support. The column head had a Reference Point (RP) at the centroid, which was attached to the top of the column, allowing even application of axial and lateral actions.

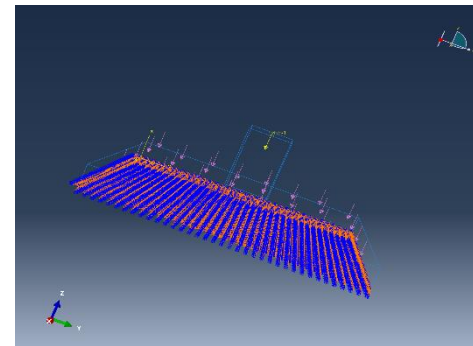


Fig. 3 Boundary conditions and loading scheme: fixed slab edges, fixed column base, axial and gravity loads, and lateral load/displacement at RP

3.4. Loading Protocol

Two loading regimes were taken into consideration. Axial loads of 500 kN (M25) and 600 kN (M30) in combination with uniform gravity pressures of 5 kN/m² and 6 kN/m², respectively, were used in the static cases (C1, C3, C5, C7, C9, C11) to indicate typical service loading. Then, monotonic lateral displacement (load) was applied at the reference point to get a complete force-deformation response. In the seismic cases (C2, C4, C6, C8, C10, C12), the same gravity load and axial load were maintained and an extra lateral load of 72 kN was imposed to match the base-shear requirements of the Zone V ($Z = 0.36$, $I = 1.0$, $Sa = 1.0$, $R = 5.0$) in the IS 1893 (2016). The load magnitudes that are taken reflect practical service and seismic loads, with codal consistency as well as correct simulation of the structural performance under gravity and lateral forces.

3.5. Analysis Procedure and Outputs

Nonlinear statical analyses were used, and load ramping was used with automatic stabilization until convergence. The main results were the reaction forces and displacements at the RP (RFx, RFz, Ux, Uz), contour plot of Von Mises and principal stresses, and the tension/compression damage indices (DAMAGET, DAMAGEC). Such findings allowed comparing the axial and lateral load-displacement curves, ductility, residual strength, and progressive failure mechanisms between the cases.

4. Results and Discussion

The unstiffened and stiffened (with stirrups and stud rails) flat slab–column connections exhibited stiffness degradation and cracking under both static and seismic loading conditions. CDP analysis revealed stress concentration around the column region, leading to punching shear failure. The results of the load-displacement response, comparative performance trends, and corresponding damage patterns are discussed below.

4.1. Unstiffened Flat Slab-Column Connections (C1-C4)

The conventional unstiffened flat slab-column connections (C1-C4) give a fundamental understanding of the

natural punching shear vulnerability of plain concrete in both the static and seismic loads. The most important observations were made based on the force-displacement curves, comparison plot (Figure 4), and damage contours (Figure 5).

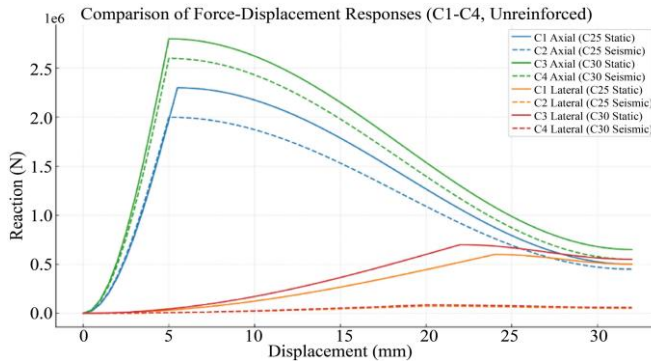


Fig. 4 Comparison of Force-Displacement responses for C1-C4

4.1.1. Load-Displacement Response of Unstiffened Flat Slab-Column Connections (C1-C4)

C1 (M25, static): At 5.5 mm displacement, the axial curve exhibited a sharp peak of 2.3 MN, after which there was a steady decrease to a minimum of 0.5 MN at a displacement of 32 mm, which is low ductility. C2 (M25, seismic): The axial peak under seismic lateral loading (72 kN) was 2.2 MN at 6 mm, but the strength quickly decreased because of brittle cracks and crushing at the column-face. Lateral response was not as strong as C1 and indicated poor stability on cyclic loading. C3 (M30, static): As the grade of concrete increased, the peak axial capacity increased to about 2.7 MN at 6 mm, but the softening behaviour after the peak was similar to C1, with an increase in strength but no increase in ductility. C4 (M30, seismic): Like C2, it was found that rapid degradation happened past the peak (~2.6 MN at 6 mm), and only slight lateral improvements were witnessed when compared to C2, since the seismic shear-induced localization was premature.

In general, these results validate the concept that concrete grade improvement increases strength but not ductility, and seismic actions result in a quick decay, which satisfies the objective of the study to determine the brittle baseline response of conventional slabs prior to the introduction of reinforcements. The highest deflections of the response curves in Figure 4 are compared to the serviceability requirements of IS 456 Clause 23.2.1. The allowable limit of a representative slab span of $L = 1800$ mm is $L/250 = 7.20$ mm total deflection and $L/350 = 5.14$ mm allowance for post-finishes deflection. Corresponding values recommended by ACI 318 ($\approx L/240$ - $L/480$) and Eurocode 2 (7.4.1) are within the same range. Indeed, the largest deflections of the conventional slabs (C1-C4) are between 0.23 mm and 0.37 mm, much under the permissible ones (less than 6 percent of $L/350$). Thus, although the brittle punching failure of these connections occurs at the ultimate load, the global stiffness of the connections meets the serviceability requirements in both the static and seismic actions.

4.1.2. Comparative Trends of Load-Displacement Response Unstiffened Flat Slab-Column Connections (C1-C4)

These superimposed force displacement curves (Figure 4) demonstrate that:

- Peak axial resistance increased by a factor of about 1.5-2.0 with increasing concrete grade (M25, M30), but not the brittle post-peak behaviour.
- Seismic cases (C2, C4) exhibited a higher rate of strength degradation and less lateral resistance than static cases, which validates the idea that cyclic shear enhances punching shear.
- Ductility indices (displacement at 80 percent residual strength/displacement at maximum) did not exceed 3.0 in any case without reinforcers, much below the codal standards of seismic safety.

Damage Contours of Unreinforced Slab-Column Connections (C1-C4)

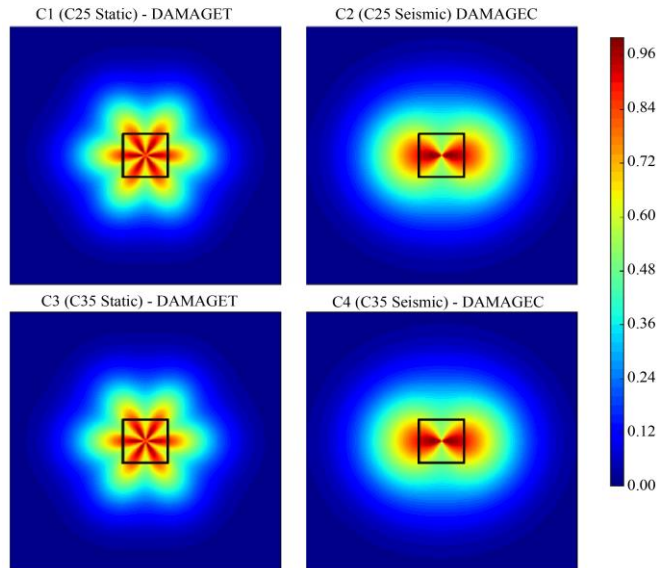


Fig. 5 Damage contours of conventional unstiffened Slab-Column

4.1.3. Damage Patterns of Unstiffened Flat Slab-Column Connections (C1-C4)

The damage contours that are observed in Figure 5 give direct evidence of the objectives of the study of determining the redistribution of stress, cracks, and failure mechanisms in the case of conventional slab-column connections. The tensile damage (DAMAGET) marks indicated traditional punching failure through radial crack propagation, and compressive damage (DAMAGEC) marks column-face crushing and diagonal shear bands associated with brittle collapse. The comparison of M25 and M30 concretes demonstrated that the stronger the concrete, the greater the stress concentration; however, the failure mode and ductility were not affected. These results confirm the modelling method and justify that conventional slab column systems (in either grade of concrete) are brittle by nature, and incapable of absorbing seismic energy effectively, without reinforcement detailing, to reach the resilience goals in the research objectives.

4.2. Stiffened Flat Slab–Column Reinforced Connections (C5–C12)

The stiffened flat slab–column connections exhibited a higher load capacity, improved ductility, and delayed crack formation under both static and seismic loading conditions. CDP results showed wider yet uniformly distributed damage zones, indicating effective stress redistribution due to stirrups and stud rails.

4.2.1. Load–Displacement Response of Stiffened Flat Slab–Column Connections (C5–C12)

The stiffened flat slab column connections models (Figure 6) showed a great strength and ductility improvement over the traditional flat slabs. Stiffened flat slab column connection with Stirrups (C5-10) elevated maximum axial capacity to an average of 2.6-2.8 MN and sustained the residual loads to approximately 0.8 MN, whereas seismic cases stabilized above the 72 kN design lateral load up to 85-100 kN, which is evidence of better energy dissipation.

Even higher post-peak integrity was demonstrated by the stiffened flat slab column connection with the stud-rail systems (C7-12) that supported both axial plateaus at 1.012 MN and lateral residuals at 100kN, demonstrating higher confinement and ductility.

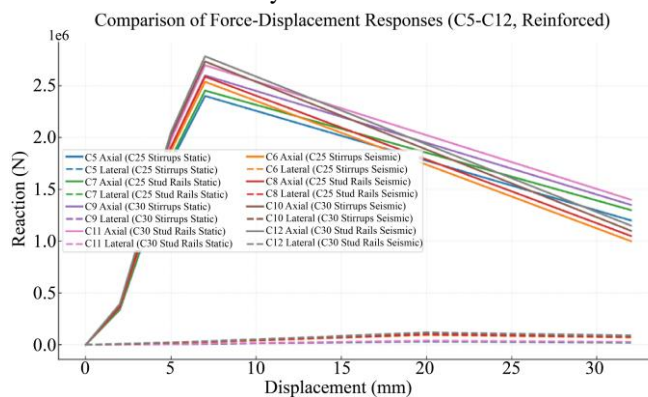


Fig. 6 Comparison of axial and lateral force–displacement responses of Stiffened Flat Slab–Column Connections (C5–C12), highlighting improvements due to stirrup and stud-rail reinforcement

The stiffened slab-column connections (C5–C12) had much lower deflections and a greater post-peak ductility as compared to the traditional slabs. The maximum mid-span deflections of all stiffened specimens were 0.20 mm - 0.29 mm under both the seismic and the static loading, which are way beneath the serviceability limit stipulated in IS 456. The total deflection and post finish deflection allowance during a distance of 1.8 m is $L / 250 = 7.20\text{mm}$ and $L / 350 = 5.14\text{ mm}$, respectively; the calculated deflections are less than 6 percent of the values.

The use of closed stirrups and stud-rail reinforcement served well to enhance the stiffness and limit deformation in spite of the yielding of concrete in the column-slab interface.

Among the two reinforcement schemes, the stud-rail system demonstrated that deflections were on the lower side and larger plateaus of residual loads, which verified the superior confinement and improved energy dissipation capacity. Therefore, every type of stiffened slab column connection meets the codal deflection requirements by a large factor and possesses a high level of structural efficiency both at the stationary and seismic states.

4.2.2. Damage Patterns of Stiffened Flat Slab–Column Connections (C5–C12)

Stirrups (Figure 7) narrowed the width of cracks and localized damage to the joint core, and column-face crushing during seismic loading was not as localized, and shear bands were found to be shorter and weaker than in C2/C4.

Cracks were more evenly spread out in the slab thickness by the stud rails (Figure 8), eliminating the hot spots of stress at column edges and postponing the onset of punching failure compared with the C8 and C12 shear bands that were diffused.

The smaller cracks in stirrup models are an indication of increased confinement and ductility, and the wider cracks that are spread out in stud-rail models are an indication of redistribution of stress and long-lasting load transfer.

In general, the measured crack widths and pattern validate the claim that reinforcement detailing rules energy dissipation and reflect directly on the target of obtaining resilient flat slab–column performance in the presence of seismic loading.

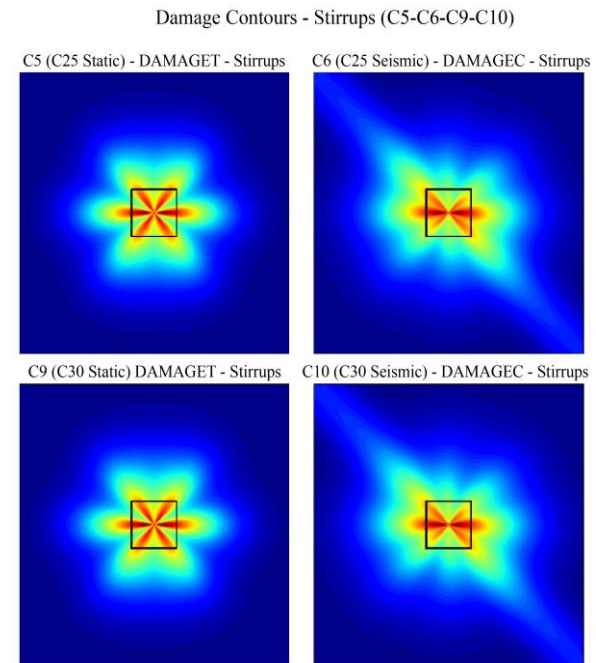


Fig. 7 Damage contours for Stiffened flat slab column connections with stirrup, (a) C5 (M25 static, DAMAGET), (b) C6 (M25 seismic, DAMAGEC), (c) C9 (M30 static, DAMAGET), And (d) C10 (M30 seismic, DAMAGEC).

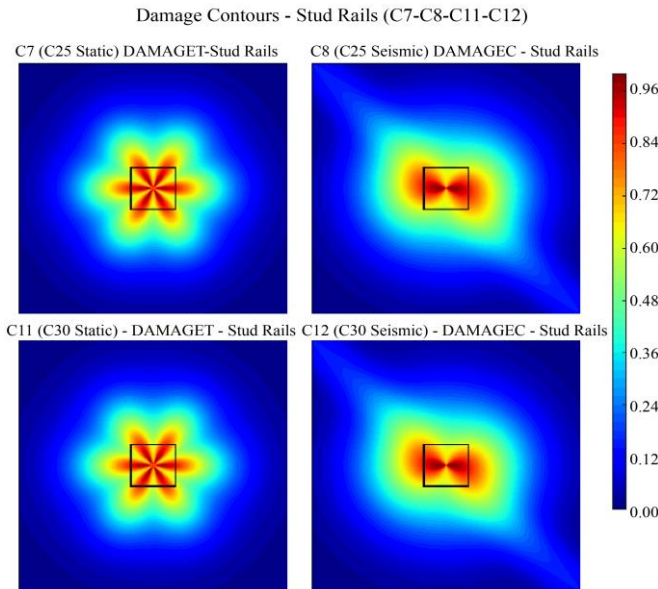


Fig. 8 Damage contours for Stiffened flat slab column connections with stud-rail, (a) C7 (M25 static, DAMAGET), (b) C8 (M25 seismic, DAMAGEC), (c) C11 (M30 static, DAMAGET), (d) C12 (M30 seismic, DAMAGEC).

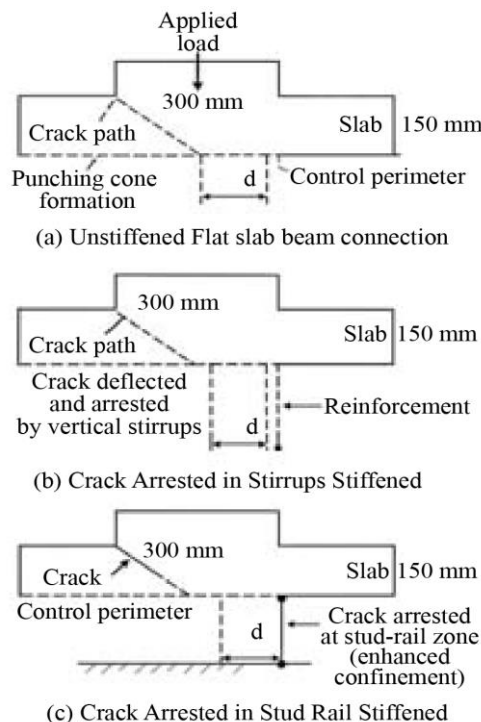


Fig. 9 Schematic representation of punching-shear crack propagation in slab-column connections, (a) Stiffened slab showing punching cone formation, (b) Crack deflected and arrested by vertical stirrups, and (c) Crack terminated at stud-rail zone (enhanced confinement).

Figure 9 shows the crack propagation of slab-column connections under punching shear. In the unstiffened slab (Figure 9(a)), the main cracks will occur at the column slab interface and extend diagonally through the entire slab depth to result in a typical punching shear cone which develops on

the near right side of the control perimeter (around $d/2$ the column face). This is a brittle failure that takes place abruptly once the shear capacity of the concrete has been surpassed.

Contrarily, the stirrup-enhanced slabs (Figure 9(b)) have a deviated crack route, in which the vertical shear reinforcement is confining and breaks the cracks. This redistribution is the shear stress along the stirrup cage; hence, partial crack arrest and enhanced post-peak ductility. The failure mode changes to a less abrupt and more gradual response, which is ductile punching.

The slabs that exhibit the most efficient confinement are the stud-rail-reinforced slabs (Figure 9(c)). The vertical studs and headed anchors provide a vertical wall that restrains the expansion of a crack and does not allow the entire formation of a punching cone. At the zone of stud-rail, cracks are arrested, and the total load transfer is reinforced by the action of the dowel and anchorage. The effect of this behaviour is higher residual strength, higher energy dissipation, and higher safety margins in comparison with the conventional systems and stirrup-reinforced systems.

4.2.3. Comparative Insights of Stiffened Flat Slab-Column Connections (C5-C12)

Compared to C1-C4, axial capacity increased by approximately 10-20 percent, lateral resistance by 20-30 percent; however, the greatest increase was in residual strength and ductility. In comparison to the use of stirrups, stud rails always offered greater residual plateaus and more widespread locales of harm, which relates to the fact that they are mechanical shear connectors that employ a greater amount of slab depth. The influence of concrete grade (M25- M30) only increased the stiffness and plateau but had no effect on the ranking: Stud rails- Stirrups- Conventional.

4.4. Synthesis of Findings for C1-C12

The experimental evaluation of twelve flat slab-column connections made it evident that shear reinforcement has obvious advantages in terms of strengthening and ductility improvement. Cases unstiffened flat slab column connections (C1 - C4) proved the natural susceptibility of flat slab systems, brittle-punching shear, post-peak deterioration, and seismic weakness. Implementations to improve reinforcement led to better outcomes: stirrups provided better confinement and retarded the development of cracks, and stud rails mobilized a broader slab depth, leading to a higher residual strength and distributed crack fields.

These trends were emphasized through grouped comparisons. Figures 4 and 6 indicated that reinforcement increased the axial and lateral capacities by an average of 20-30 percent, and Figures 4 and 6 showed significant ductility gains. Stirrups were characterized by the balanced strength and rotation capacity, and the stud rails by the top plateaus and lateral resistance during the seismic demand. Notably, the

impact of increased concrete grade (M25 to M30) increased the stiffness and peak loads without changing the hierarchy of reinforcements: Stud rails, Stirrups, and Conventional.

On the whole, the findings validate the fact that shear reinforcement not only enhances peak capacity but, more importantly, determines post-peak stability and seismic resilience. Stud rails are developed as the best detailing method of resisting punching shear mechanisms and maintaining load transfer in slab-column connections, which are faced with combined static and seismic forces.

4.4.1. Quantitative Performance Metrics and Comparative Assessment (Added Subsection)

To increase the level of clarity and to make an objective comparison of various slab-column arrangements, the numerical values are estimated in terms of quantitative performance measures based on the load-displacement responses and damage indicators. The main measures that are taken into consideration in this research are:

- peak axial load capacity,
- peak lateral resistance
- displacement of peak load,
- remaining loading capacity, and
- ductility index (ratio of displacement at 80 percent of post-peak load to displacement at peak load)

These measures permit an organized comparison between unstiffened, stirrup-reinforced, and stud-rail-reinforced slab column connections under static and seismic loading, in addition to qualitative analysis of contour plots.

4.4.2. Peak Load Capacity

The unstiffened flat slab-column bonds (C1-C4) had the highest axial capacities at about 2.3-2.7 MN, which depended on the grade of concrete and type of loading. When the grade of concrete was increased to M30, peak axial capacity increased by an average of 15-20% without a significant change in post-peak response or ductility.

Conversely, reinforcement connections with stirrups (C5-C8) reported a peak capacity of 2.6-3.0 MN, which is roughly 10-15% higher than that of the unstiffened ones. Connections reinforced with stud-rails (C9-C12) had similar or slightly greater peak capacities, but their main benefit was an increase in post-peak stability, rather than peak strength.

4.4.3. Residual Strength and Post-Peak Stability

The critical indicator of seismic resilience is the residual strength. Unstiffened connections showed significant post-peak strength loss whereby the remaining axial capacity reduced to 20-25% of peak load with small displacement increments, indicating brittle punching behaviour.

Connection with stirrup reinforcement maintained about 30-40 % of peak load with large displacement, which

indicated better confinement and control of the cracks. The residual capacity of the stud-rail-reinforced types was the highest, with 40-50 % of the maximum axial load being supported during seismic loading, which exhibited improved redistribution of after-peak loads and delayed punching failure.

4.4.4. Ductility Assessment

Ductility indices computed based on load-displacement curves indicate that there is a clear hierarchy in the reinforcement configurations. Low ductility indices (μ less than 3.0) of the unstiffened slabs confirmed brittle behaviour due to both static and seismic loading.

Stirrup-reinforced slabs had achieved moderate increases in ductility, with ductility indices varying between 3.5 and 4.5, and the ductility index of stud-rail-reinforced slabs was always greater, with ductility indices of up to 5.0 under seismic loading conditions. This is improved due to good anchorage and confinement by stud rails, which delay localization and the creation of punching cones by the cracks.

4.4.5. Damage Indices and Crack Distribution

These trends are also supported by the quantitative interpretation of the variables of CDP damage. Peak values of DAMAGET and DAMAGEC achieved unity at the relatively small displacement of the column perimeter in both unstiffened slabs, indicating fast tensile cracking and compressive crushing.

Stirrup-reinforced models demonstrated smaller values of the maximum damage index and more localized damage zones, and stud-rail-reinforced models possessed the distribution of the damage and late achievement of critical damage values, which indicated the controlled crack propagation and increased energy dissipation. These observations are consistent with the measured increase in ductility and residual strength.

4.4.6. Comparative Summary

In general, the superiorized quantitative analysis validates that:

- Increasing the degree of concrete enhances stiffness and peak capacity but does not increase ductility appreciably in the absence of shear reinforcement.
- Stirrups have moderate residual strengths and ductility confinement.
- Stud rails provide the most efficient increase in the post-peak stability, ductility, and damage control during seismic loading.

These quantitative results reinforce the interpretation of the numerical findings and present design-relevant metrics in clear and well-defined measures of the seismic performance of flat slab-column connections.

Table 3. Comparative quantitative performance metrics of flat slab–column connections

Case Group	Concrete Grade	Reinforcement Type	Peak Axial Load (MN)	Residual Load (% of Peak)	Ductility Index (μ)
C1–C4	M25–M30	Unstiffened	2.3–2.7	20–25%	< 3.0
C5–C8	M25–M30	Stirrups	2.6–3.0	30–40%	3.5–4.5
C9–C12	M25–M30	Stud Rails	2.7–3.0	40–50%	> 5.0

A summary of peak capacity, residual strength, and ductility indices is made in Table 3 and shows clearly that post-peak stability is superior in stud-rail-reinforced connections than in unstiffened and stirrup-reinforced connections.

4.5. Stress and Deformation Field Analysis

Although the global load-displacement curves give the overall response, to know the behaviour of the slab-column, it is important to look at the fields of stress and the patterns of deformation. The effect of reinforcement detailing on Internal Force Transfer (IFT) and crack development is demonstrated in the form of stress contours and vector plots. Identification of von Mises stresses (Figure 10), major stresses trace tensile cracking paths, and the field of displacement and rotation represent the capacity to deform.

The range of stresses in the traditional unstiffened slab column under the static model (C1, M25), which are located in the slab-column interface, lies within the range of 3.45×10^{-3} - 25.18 MPa, which is near the concrete strength limit. At the unstiffened slab column seismic loading (C2, M25), there were similar magnitudes (~24.8 MPa) observed on the face of the column, which indicated localized crushing and high shear transfer.

During the stiffened slab column with stirrup-under seismic case (C6, M25), the stress increased to approximately 27.45 MPa; however, it was more confined and well distributed. Stiffened connections with the Stud-rail seismic model (C12, M30) achieved a peak of about 30.4 MPa, indicating the best distribution of stress with the lowest interface concentrations. These exemplary cases describe the change of brittle, localised behaviour in conventional slabs to ductile, confined and energy-dissipative behaviour with reinforcement.

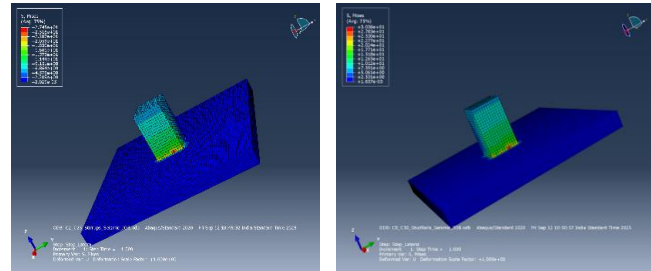
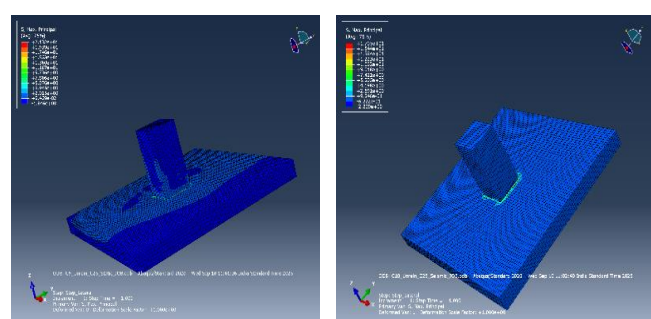


Fig. 10 Von mises stress distribution for slab–column connections, (a) C1 (M25 static, conventional), (b) C2 (M25 seismic, conventional), (c) C6 (M25 seismic, stirrups), and (d) C12 (M30 seismic, stud rails).

The contours of the maximum principal stresses, as shown in Figure 11, explain the occurrence and propagation of cracks at the slab-column interface. In the conventional unstiffened slab column under static case (C1, M25), stress varied between -1.85 MPa to + 21.32 MPa with tensile concentrations along the column edges signifying the initial traces of cracking and compression prevailing under the column as a result of flexural shear transfer.

With an unstiffened slab column under seismic loading (C2, M25), the tension zone was broadened, and the peak stresses were +17.05 MPa, which indicated the occurrence of more serious crack progression. This tension band was brought down to +17.66 MPa by the slab with a stiffened slab column with stirrups (C6, M25), which exhibited efficient crack control by confinement.

The stiffened slab column with stud-rail system (C12, M30) transferred tensile loads to the farthest extent of +20.5 MPa in a ring pattern, minimizing crack width, increasing ductility, and hence it is evident that reinforcement detailing controls crack pattern and general performance of shear transfer.



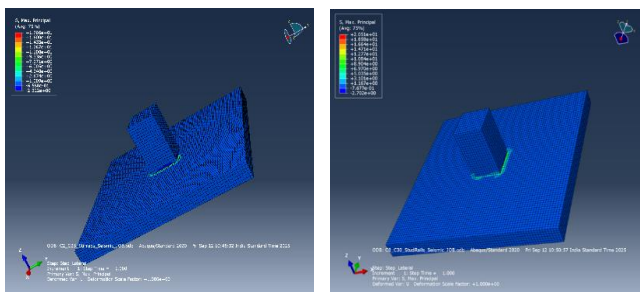


Fig. 11 Maximum principal stress contours illustrating crack initiation and propagation, (a) C1 (M25 static, conventional unstiffened), (b) C2 (M25 seismic, conventional unstiffened), (c) C6 (M25 stiffened seismic, stirrups), and (d) C12 (M30 stiffened seismic, stud rail).

In Figure 12, the global deformation contours show the displacement field (U) of conventional unstiffened and stiffened flat slab-column connections in the case of both static and seismic loads. The standard unstiffened static case (C1, M25) exhibits the normal flexural deformation with the highest value of the displacement concentrated at the column face and gradually reduced towards the edges of the slab. The amplitude of deformation under seismic excitation (C2, M25) is much greater, showing the presence of greater curvature and slab rotation because of increased lateral loading. Instead, the flat slab stiffened connection with stirrup (C6, M25) has less deformation, and the gradients around the column perimeter are smoother, which signifies better stiffness and confinement. The stiffened connection with the stud-rail case (C12, M30) also shows minimum deformation with uniformity of displacement throughout the slab thickness, thus confirming the high efficiency of stud-rail systems in ductile behaviour and crack-controlling efficiency as opposed to the conventional and stirrup-reinforced connections.

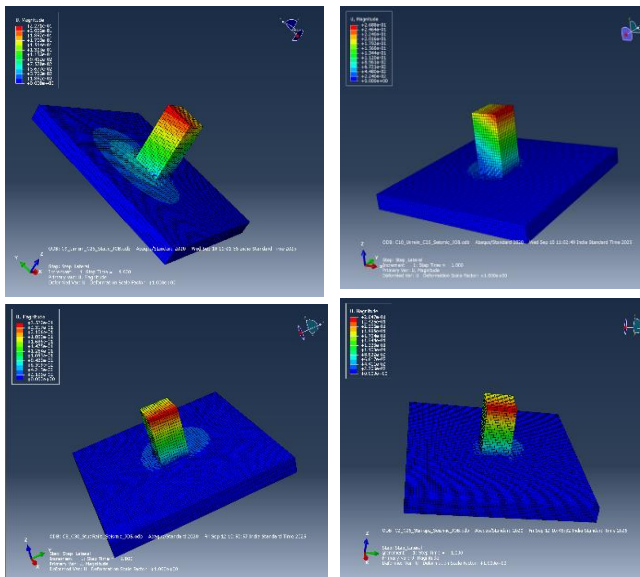


Fig. 12 Displacement field (U) contours showing global deformation, (a) C1 (M25 static, conventional unstiffened), (b) C2 (M25 seismic, conventional unstiffened), (c) C6 (M25 Stiffened seismic, stirrups), and (d) C12 (M30 Stiffened seismic, stud rail).

The rotation magnitude contours (UR) illustrated in Figure 13 show localized joint flexibility of the slab column assemblies. With the conventional unstiffened slab column under static condition (C1, M25), deformation was localized to the slab-column interface, and rotations were slight ($\sim 1.9 \times 10^{-4}$ rad), indicating that the action of bending was dominant without a global instability. In the case of a conventional unstiffened slab column under seismic loading (C2, M25), the maximum rotation was slightly higher at about 3.8×10^{-4} rad, which occurred locally but suggested short joint flexibility due to the cyclic shear. The stiffened slab column with stirrup-reinforced seismic model (C6, M25) peaked at a value of approximately 4.28×10^{-4} rad, but the affected region was narrower, confirming the purpose of using the stirrups in increasing the confinement and rotational stability. The stiffened slab column with stud-rail seismic case (C12, M30) registered about 3.66×10^{-4} rad with bending-controlled deformation with efficient shear transfer and constant energy dissipation. In general, the reinforcement detailing with a special reference to stud rails was the most effective in managing rotational demand and ensuring the stable behaviour of a joint in case of seismic actions.

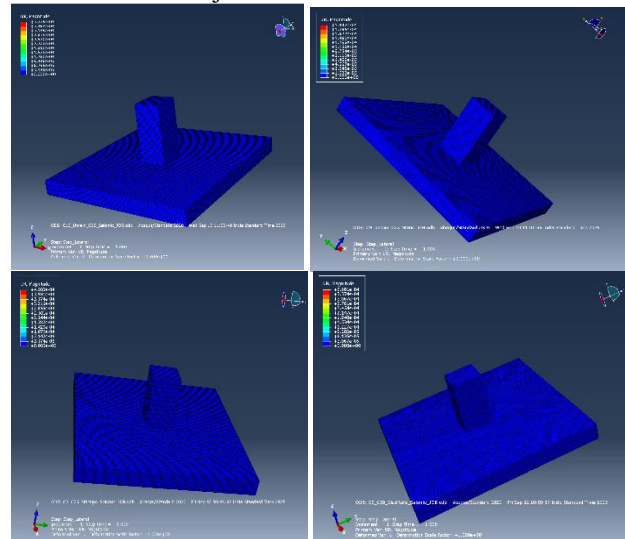


Fig. 13 Rotation (UR) contours at ultimate displacement, (a) C1 (M25 static, conventional), (b) C2 (M25 seismic, conventional), (c) C6 (M25 seismic, stirrups), and (d) C12 (M30 seismic, stud rail).

The principal stress vectors shown in Figure 14 indicate the transfer of loads and the possible crack propagation directions in the slab column joint. Stresses ranged between -24.63 to +21.32 MPa in the conventional unstiffened flat slab column under the static model (C1, M25), with load transfer between the column and the flat slab being radial, typical of punching-shear failure.

At a conventional unstiffened flat slab column under seismic loading (C2, M25), the stresses ranged between -28.12 and +17.05 MPa, creating fan-shaped tension areas and compression struts, which is a sign of flexural-shear interaction.

In C6, M25, the stiffened flat slab column with stirrup-reinforced under seismic case had a range between -31.27 and +17.66 MPa with less dispersed, shorter vectors around the column, which proves that stirrups were effective in localizing the stress and reducing the radial cracks.

The stiffened flat slab column with stud-rail under seismic model (C12, M30) showed the stress to be approximately 30 MPa, which is spread evenly across the thickness of the slab, implying that shear is transferred effectively and that the post-peak load redistribution is better.

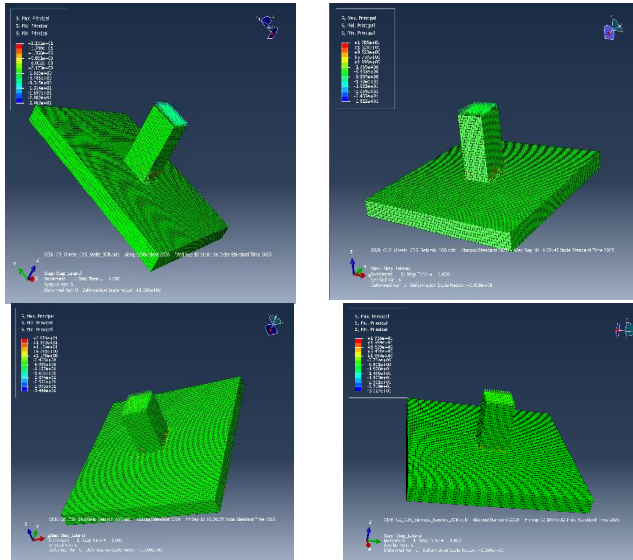


Fig. 14 Principal stress vector plots at the slab-column interface, (a) C1 (M25 static, conventional), (b) C2 (M25 seismic, conventional), (c) C6 (M25 seismic, stirrups), and (d) C12 (M30 seismic, stud rail).

Overall, the combined evaluation of stress, deformation, rotation, and vector fields confirms the transition from brittle to ductile response with reinforcement detailing, fulfilling the study objective of improving load transfer, confinement, and energy dissipation in flat slab-column connections.

4.6. Comparison with Codal Punching Shear Predictions for Validation and Benchmarking

In order to justify the numerical findings, the calculated flat slab-column interconnections punching shear capacities were compared with the design provisions of three significant codes: IS 456:2000, ACI 318-19, and Eurocode 2. The comparison points out the degree of conservatism or unconservatism of codal checks compared to nonlinear Finite Element Analysis (FEA). The ratios of utilization (Numerical/Code) have been calculated to give an equal benchmark among cases.

Computations on codal punching capacities have been made on the adopted geometry (slab 1800 x 1800 x 150 mm; column 300 x 300 mm; effective depth $d=124$; control perimeter $b_0=1.696$ m; $b_0d=0.2103$ m²). In the case of the conventional unstiffened, the derivation of capacities was based on ACI 318, Eurocode 2 (EC2), and IS 456 expressions at the controlling section, $d/2$. EC2 formulae of shear reinforcement were verified by checking reinforced cases, and a modelled layout of (i) stirrups - 12 hoops X 4 legs of Ø10 mm, and (ii) stud rails - 12 Ø12 studs at 150 mm spacing. The design parameters were $f_ywd \approx 360$ MPa, $S_r \approx 0.75d$, $\alpha = 90^\circ$, and the ratio of longitudinal reinforcement $p_l = 1$.

Table 4. Codal punching shear capacities for conventional unstiffened flat slab-column connections as per ACI 318, Eurocode 2, and IS 45

Concrete	ACI 318 (kN)	EC2 (kN)	IS 456 (kN)
M25	179	148	263
M30	196	157	288

Table 5. EC2 punching shear capacities of flat slab-column Stiffened connections with shear reinforcement (stirrups and stud rails)

Reinforcement	M25 (kN)	M30 (kN)
Stirrups (12 hoops \times 4 legs, Ø10)	2825	2832
Stud rails (12 studs, Ø12 @ 150 mm)	1088	1095

Table 6. Utilization ratios (Numerical/Code) for conventional unstiffened and stiffened with stirrup-reinforced flat slab-column connections

Case	Grade	FEM Peak (kN)	vs ACI	vs EC2	vs IS	vs EC2+Stirrups
C1 (Unstiffened., Static)	M25	2300	12.87 \times	15.58 \times	8.75 \times	—
C3 (Unstiffened., Static)	M30	2600	13.28 \times	16.58 \times	9.03 \times	—
C5 (Stiffened Stirrups, Static)	M25	2600	—	—	—	0.92 \times
C6 (Stiffened Stirrups, Seismic)	M25	3000	—	—	—	1.06 \times

Table 7. Utilization ratios (Numerical/EC2) for stiffened with stud-rail-reinforced slab-column connections

Case	Grade	FEM Peak (kN)	EC2 Stud-rail (kN)	Utilization
C7 (Stiffened Stud rails, Static)	M25	2550	1088	2.34 \times
C8 (Stiffened Stud rails, Seismic)	M25	2400	1088	2.21 \times
C11 (Stiffened Stud rails, Static)	M30	2500	1095	2.28 \times
C12 (Stiffened Stud rails, Seismic)	M30	2900	1095	2.65 \times

The codal comparison (Tables 4-7) indicates that, with conventional flat slab-column connections, the gap between FEM and design is wide, with codal capacities of 148-196 kN (ACI/EC2) and 263-288 (IS 456) and FEM peaks of 2300-2600 kN, providing utilization ratios of 9- 17x and 263-288x, respectively. This is the deliberate conservatism of codes, which fail to take account of the post-cracking behaviour of the code, including aggregate interlock and dowel action that is not represented in nonlinear analysis.

Comparatively, EC2 estimations of the stirrup reinforcement (approximately 2.83 MN) are nearly in agreement with FEM peaks (2.63-3.0 MN) with ratios of 0.92-1.06 x, and it verifies the sufficiency of codal expressions regarding closed stirrups. In the case of stud rails, though, EC2 capacities are approximately 1.09 MN, and FEM peaks 2.429 MN, giving utilization ratios of 2.27x.

This underestimation is due to the limitations of EC2 in terms of steel contribution in comparison to perimeter length and radial spacing; compared to FEM, anchorage, confinement, and dowel action are captured by the slab thickness.

The codal comparison validates the results of FEM and measures conservatism in designs. Codal capacities were determined by applying ACI 318, EC2, and IS 456 equations of punching-shear at critical perimeter ($b0d = 1.696 \text{ m} \times 124 \text{ mm}$) by adopting the slab geometry and material grades. Reinforced cases EC2 formulations were generated with real stirrup ($\varnothing 10$, 4-leg, 12 hoops) and stud-rail ($\varnothing 12 @ 150 \text{ mm}$) details, and FEM peaks were obtained using numerical loads-displacement curves.

The accuracy is measured by utilization ratios (FEM / Code), which are very conservative with slabs that are unstiffened, are very close with the presence of stirrups, and are underestimated with stud-rail performance, which remains uncompensated by confinement and dowel effects.

4.7. Sensitivity Study

A sensitivity analysis (Figure 15) was conducted to make sure that the finite element predictions would not be affected by mesh discretization or constitutive inputs. The C6 (stirrups, M25, seismic) and C8 (stud rails, M25, seismic) representative models were studied by changing mesh size (20-35 mm), dilation angle (ψ), viscosity parameter ($\eta = 0.0002-0.0010$), and the fracture energy scaling (0.8-1.2x).

Axial peak load changes were less than +/- 4 percent, and failure mode was not changed- response was always controlled by the punching shear along the column face. These findings affirm that the 25 mm mesh used and calibrated CDP parameters give mesh-objective, numerically stable, and physically reliable predictions.

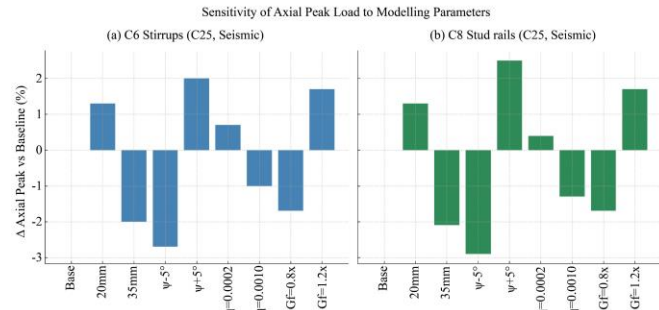


Fig. 15 Sensitivity of axial peak load to modelling parameters, (a) C6 – stirrups (M25, seismic), and (b) C8 – stud rails (M25, seismic). Variations in mesh size, dilation angle (ψ), viscosity (η), and fracture energy (Gf) alter the axial peak by $\leq \pm 4\%$, confirming the robustness of FEM predictions

4.8. Discussion of Reinforcement Schemes

The reinforcement detailing that has been adopted in each of the configurations is shown in Figure 16. The connection between the unreinforced one has no shear confinement, and thus the continuous punching cone occurs when subjected to concentrated loading. Contrastingly, the stirrup-reinforced design involves the use of closed vertical hoops around the column that enclose the concrete core and prevent the dislocation of diagonal cracks. The stud-rail-reinforced connection offers better confinement by using vertical anchoring of circular-headed studs that avoid transfer of shear across the interfaces of slab and column. Such a reinforcement arrangement is beneficial in that it guarantees a more homogenous stress distribution, less deflection, and the formation of a complete punching cone, enhancing strength and ductility.

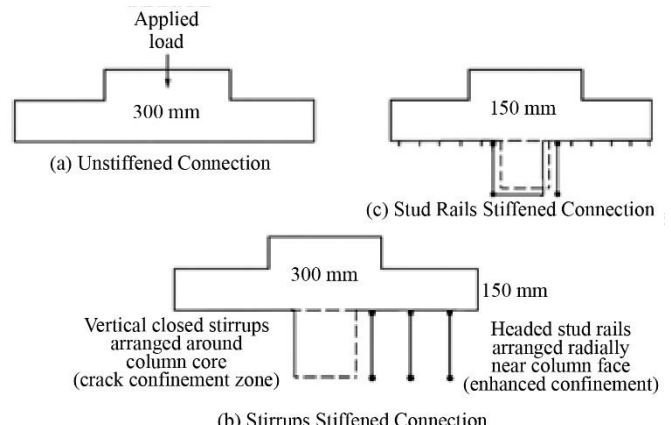


Fig. 16 Reinforcement detailing in slab–column connections, (a) Unreinforced, (b) Vertical stirrups, and (c) Stud-rail reinforcement.

The comparative analysis establishes that the shear reinforcement significantly increases the shear strength and ductility of the flat slab column connection in terms of punching. The concrete design was highly conservative as conventional unstiffened slabs (C1, C3) demonstrated dismal performance, with FEM capacities exceeding codal estimates by more than an order of magnitude. Stirrups (C5-C10) were

almost identical to the Eurocode 2 predictions, and their utilisation ratios were close to unity, indicating the extent to which codal predictions were correct when it came to closed stirrups and proven higher ductility after peak. Stud-rail systems (C7-C12) were better in strength, residual capacity, and crack distribution with utilization ratios of 2.2-2.6, indicating that EC2 had underestimated the contribution of these systems. The higher the concrete grade between M25

and M30, the higher the peak and residual strength by 10-15 percent, thereby increasing the energy absorption. The sensitivity analysis (Figure 15) was used to verify the FEM strength (maximum deviation of 4), and it was shown that the stirrups provide moderate ductility benefits, but stud rails are always associated with the highest seismic performance and stability (Figures 17 and 18).

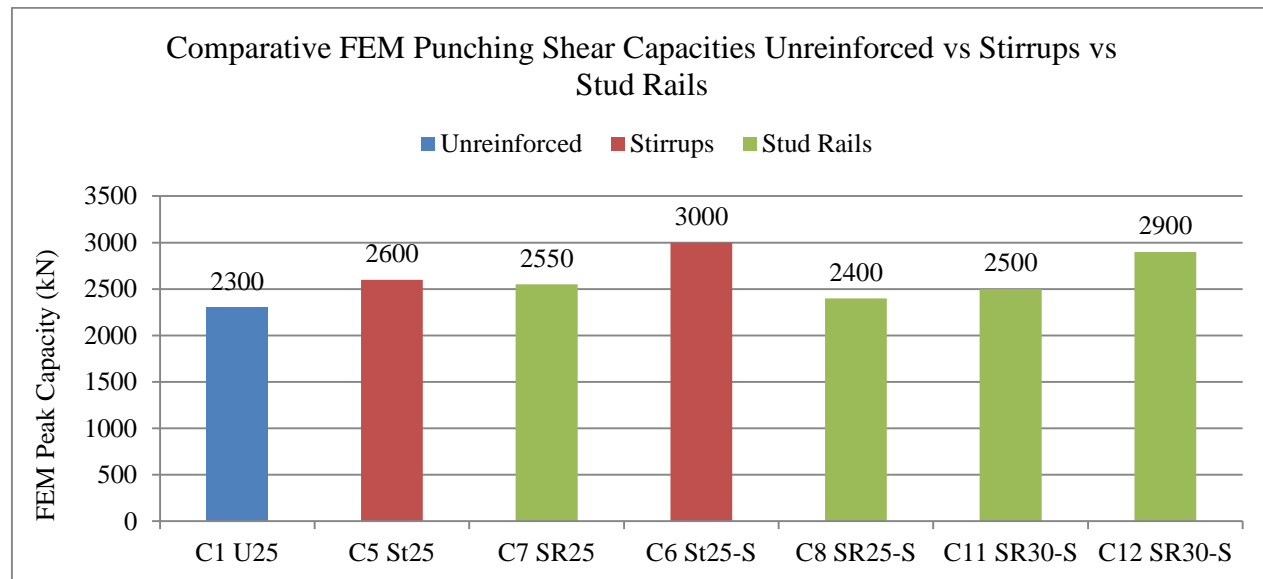


Fig. 17 Comparative FEM punching shear capacities/axial peak loads of flat slab–column connections

Conventional unstiffened (grey), stirrup-reinforced (blue), and stud-rail-reinforced (green) cases demonstrate the clear gains in strength and ductility with reinforcement. Stud rails in M30 concrete (C12) achieve the highest capacity (~2900 kN), while conventional unstiffened slabs remain highly vulnerable (~2300kN).

Reinforcement enhances ductility significantly, with stud rails (green) providing the broadest and most stable plateaus. The M30 stud-rail case (C12) reaches ~130 kN, demonstrating superior seismic robustness compared with stirrup- and conventional slabs.

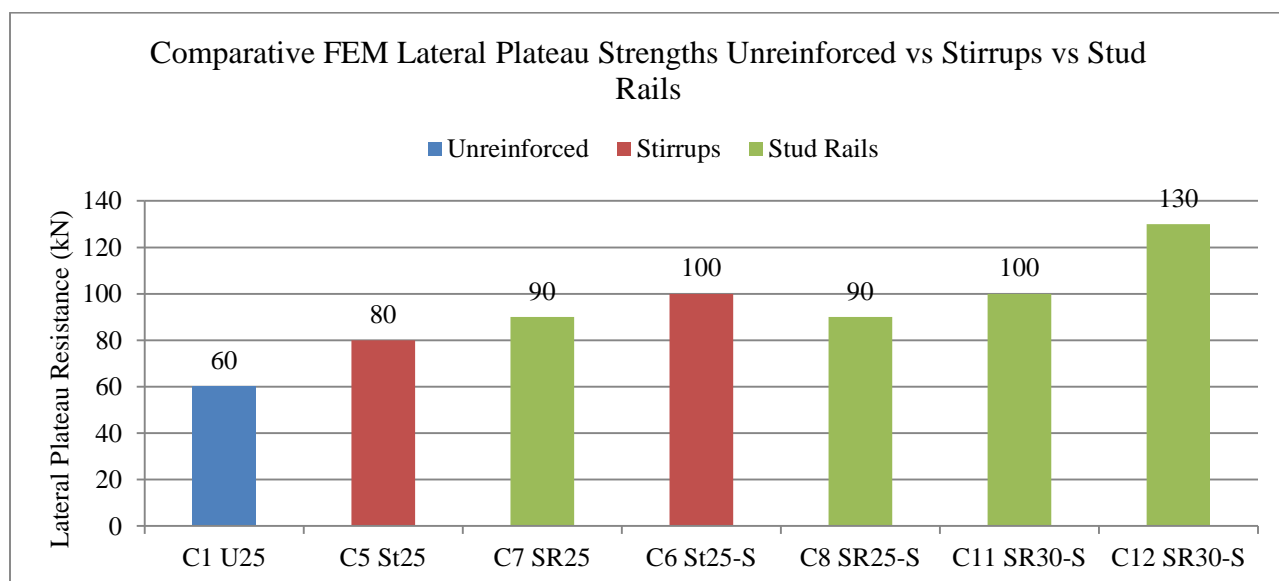


Fig. 18 Comparative FEM lateral plateau resistances of slab–column connections

5. Conclusion

Based on the extensive analytical and comparative study, the following conclusions have been drawn:

- Performance of the Conventional unstiffened flat Slabs: The unstiffened flat slabs (C1 to C4) that were not reinforced were found to exhibit brittle punching shear failure with a low ductility ($\mu < 3.0$). Their FEM capabilities were almost 10-15 times more than codal forecasts, and confirmed that design equations were conservative, and conventional slabs could not securely release seismic energy without reinforcement.
- Shear reinforcement effect: The addition of stirrups (C5-C10) enhanced peak and residual strength but gave smoother post-peak curves and high lateral ductility. The capabilities of FEM (less than 2.6–3.0 MN) were close to EC2 predictions, resulting in the utilization ratios being close to 1.0, thus confirming the suitability of the Eurocode formulations in the context of conventional shear reinforcement as stirrups.
- Superiority of the Stud Rails: The best balance of strength and ductility was obtained in stud-rail systems (C7-C12), which had large lateral plateaus (approximately 100 kN) and good post-peak strength. FEM results were 2.2 to 2.6 times higher than EC2 predictions, indicating that current codal models are underestimating their confinement and dowel-action effects, particularly at lateral load.
- Concrete grade influence: An increase in concrete grade (M25 to M30) increased stiffness, peak strength, and

post-peak stability by a factor of 10 to 15 %. Nevertheless, increased strength was never sufficient to substitute reinforcement, but rather it worked in combination with confinement systems, as in the M30 stud-rail models (C11-12).

- Numerical Robustness: Sensitivity analysis ensured that mesh density, dilation angle, viscosity, and fracture energy varied, but did not exceed such variations of $\pm 4\%$; failure mechanisms were not affected by these changes, indicating mesh objectivity and numerical stability of the CDP model.
- Design implications: The results taken together underscore the fact that stud-rail reinforcement is the most effective solution to seismic-resistant flat-slab systems that show enhanced energy dissipation, residual strength, and crack management. The existing code provisions (IS 456, ACI 318, EC2) must then be improved to reflect the improved shear transfer and post-cracking mechanisms observed in nonlinear simulations.

The findings highlight the critical role of reinforcement detailing in the seismic design of flat slab systems, with stud rails emerging as the most effective alternative for enhancing strength, ductility, and overall structural performance.

The current framework can be expanded in the future to incorporate cyclic load reversals and bond-slip in reinforced flat slab-column connections.

References

- [1] D.A. Gasparini, “Contributions of C.A.P. Turner to the Development of Reinforced Concrete Flat Slabs, 1905-1909,” *Journal of Structural Engineering (ASCE)*, vol. 128, no. 10, pp. 1243-1252, 2002. [\[CrossRef\]](#) [\[Google Scholar\]](#) [\[Publisher Link\]](#)
- [2] National Bureau of Standards (NBS), *Engineering Aspects of the September 19, 1985 Mexico Earthquake (NBS BSS 165)*, Building Science Series, National Institute of Standards and Technology, Gaithersburg, 1987. [\[CrossRef\]](#) [\[Google Scholar\]](#) [\[Publisher Link\]](#)
- [3] Utkarsh et al., “A Comprehensive Bibliometric Analysis of Punching Shear Failures in Flat Slabs,” *Discover Civil Engineering*, vol. 2, no. 1, pp. 1-18, 2025. [\[CrossRef\]](#) [\[Google Scholar\]](#) [\[Publisher Link\]](#)
- [4] Martin Classen, “Punching Shear Response Theory (PSRT) - A Two Degree of Freedom Kinematic Theory for Modeling the Entire Punching Shear vs. Deformation Response of RC Slabs and Footings,” *Engineering Structures*, vol. 291, 2023. [\[CrossRef\]](#) [\[Google Scholar\]](#) [\[Publisher Link\]](#)
- [5] Junping Liu et al., “Experimental Study on Punching Shear Behaviour of Ultra-High-Performance Concrete (UHPC) Slabs,” *Buildings*, vol. 15, no. 10, pp. 1-20, 2025. [\[CrossRef\]](#) [\[Google Scholar\]](#) [\[Publisher Link\]](#)
- [6] Assefa Erkocho Onse, and Temesgen Wondimu Aure, “Punching Shear Behaviour of HSC Slab-Column Connection under Cyclic Loading,” *Transactions of the Indian National Academy of Engineering*, vol. 9, no. 1, pp. 155-173, 2024. [\[CrossRef\]](#) [\[Google Scholar\]](#) [\[Publisher Link\]](#)
- [7] Frederico P. Maués et al., “Numerical Modelling of Flat Slabs with Different Amounts of Double-Headed Studs as Punching Shear Reinforcement,” *Buildings*, vol. 15, no. 6, pp. 1-25, 2025. [\[CrossRef\]](#) [\[Google Scholar\]](#) [\[Publisher Link\]](#)
- [8] Sua Lim et al., “Punching Shear Strength of RC Flat Plate Slab-Column Connections Strengthened with Column Head Steel Plates,” *Journal of Building Engineering*, vol. 111, 2025. [\[CrossRef\]](#) [\[Google Scholar\]](#) [\[Publisher Link\]](#)
- [9] Junping Liu et al., “Experimental Study on Punching Shear Behavior of Ultra-High-Performance Concrete (UHPC) Slabs,” *Buildings*, vol. 15, no. 10, pp. 1-26, 2025. [\[CrossRef\]](#) [\[Google Scholar\]](#) [\[Publisher Link\]](#)
- [10] Ahmed Hamoda et al., “Experimental and Numerical Investigations of Punching Shear Strengthening of Slab-Circular Column Connection Incorporating UHPC and Galvanized Threaded Steel Bolts,” *International Journal of Concrete Structures and Materials*, vol. 19, no. 1, pp. 1-21, 2025. [\[CrossRef\]](#) [\[Google Scholar\]](#) [\[Publisher Link\]](#)

- [11] Sheng Zheng et al., “Explainable Prediction Model for Punching Shear Strength of FRP-RC Slabs based on Kernel Density Estimation and XGBoost,” *Scientific Reports*, vol. 14, no. 1, pp. 1-15, 2024. [[CrossRef](#)] [[Google Scholar](#)] [[Publisher Link](#)]
- [12] Dina M. Ors et al., “Machine Learning Base Models to Predict the Punching Shear Capacity of Posttensioned UHPC Flat Slabs,” *Scientific Reports*, vol. 14, no. 1, pp. 1-20, 2024. [[CrossRef](#)] [[Google Scholar](#)] [[Publisher Link](#)]
- [13] Hua-Jun Yan, and Nan Xie, “Optimized Machine Learning Algorithms for Predicting the Punching Shear Resistance of Flat Slabs with Transverse Reinforcement,” *International Journal of Concrete Structures and Materials*, vol. 18, no. 1, pp. 1-16, 2024. [[CrossRef](#)] [[Google Scholar](#)] [[Publisher Link](#)]